Arm-First Synthesis of Star Polymers with Polywedge Arms Using Ring-Opening Metathesis Polymerization and Bifunctional Crosslinkers

Robert Learsch,[1] Garret M. Miyake [1,2,3]

[1]Materials Science and Engineering Program, University of Colorado Boulder, Boulder, Colorado 80309
[2]Department of Chemistry and Biochemistry, University of Colorado Boulder, Boulder, Colorado 80309
[3]Department of Chemistry, Colorado State University, Fort Collins, Colorado 80523
Correspondence to: G. M. Miyake (E-mail: garret.miyake@colostate.edu)

ABSTRACT: This work presents a two-step, one-pot process to make star polymers with polywedge arms. In a one-pot reaction, after the polywedge arms are synthesized, crosslinker species are added to the reaction, rapidly forming star polymers. Crosslinker species with different degrees of conformational freedom were designed and synthesized and their capacity to generate star polymers was evaluated. Mass conversions up to 92% and stars with up to 17 arms were synthesized with the most rigid crosslinker. The effects of arm molecular weight and molar ratio of crosslinker to arm on mass conversion and arms per star were explored further. Finally, the size-molecular weight scaling relationship for polywedges with linear and star architectures was compared, corroborating theoretical results regarding star polymers with arms much larger than their core. © 2018 Wiley Periodicals, Inc. J. Polym. Sci., Part A: Polym. Chem. **2018**, *00*, 000–000

KEYWORDS: arm-first; conformational analysis; high molecular weight polymers; ROMP; star polymers

INTRODUCTION Star polymers consist of a chemically distinct core from which many (3 to 100+) polymer chains extend and form a spherical structure.[1–5] The star architecture was first accessed via anionic polymerization methods[6] and has been extensively studied as a method for affecting changes in materials properties while maintaining the chemical composition of the constituent arms.[7] To access these distinct materials properties, star polymers combine the chemical functionality of their arms with a spherical, compact shape, a high density of end-groups, and a core–shell structure similar to that of micelles.[7–9] The potential for controlled synthesis to modify the properties of the macromolecules has increased interest for star polymers in sophisticated applications. Star polymers have been developed and used as additives for improving oil viscosity,[10] biomedical devices for drug delivery,[8,11,12] unimolecular containers for nanomaterials,[13,14] and films with improved self-assembly.[15]

There are three prominent strategies for star polymer synthesis: arm-first,[9,16–18] core-first,[11,14,19] and grafting-onto.[20–22] Arm-first synthesis aims to grow polymer arms and then crosslink them to form a core; the core-first method relies on a multi-functional initiator from which the polymer arms are grown; the grafting-onto approach reacts polymer arms with a core which have both been prepared independently. For all three methods, control over the molecular weight (MW) and chemical composition of the arms and the number of arms per star is paramount to the synthesis of star polymers that successfully execute their intended function.[10,23,24] For example, increases in the MW of the polymer arms lead to a transition from Newtonian to viscoelastic rheological behavior.[25] The number of arms dictates the number of end-groups present and magnitude of star-star interactions.[26,27]

Synthetic control of the composition and length of the polymer arms can be accessed through controlled polymerization methods such as atom transfer radical polymerization (ATRP)[16,18,28] and reversible addition-fragmentation transfer (RAFT) radical polymerization[29] or living polymerization methods such as anionic,[6] cationic,[30] ring-opening polymerization (ROP),[31–33] and ring-opening metathesis polymerization (ROMP).[34–36] ROMP can produce polymers with large MWs and extremely narrow molecular weight distributions (Đ) and is used to synthesize polymers with unique characteristics. ROMP is compatible with sophisticated monomers such as macromonomers which form bottle-brush polymers[37–39] and dendritic wedge-like monomers which form

Additional Supporting Information may be found in the online version of this article.

polywedges.[40–42] These polymers are designed to have very high critical molecular weights and avoid chain entanglement. Such polymers act as rigid rods in solution and exhibit low glassy and plateau moduli;[41,43] behavior that is expected of polymers with low chain entanglement.[44,45]

Previously, modified ruthenium-based catalysts have been used in the core-first synthesis of 3-arm star polymers.[46] In addition, traditional ROMP catalysts can be employed to synthesize star polymers from bottle-brush polymers through the arm-first approach.[34,35] One method to access the bottle-brush architecture is through the polymerization of macro-monomers, polymer chains terminated with *exo*-norbornene, and polymerized *via* ROMP to form graft copolymers.[34,35,38,39] In comparison, polywedges of the same length benefit from decreased dispersity and molecular weight due to the simplicity of their monomers.[40] However, there is no precedence for creating star polymers with polywedge arms. A method to reliably make star polymers from polywedge arms will enable the study of how star polymer behavior deviates from that of their linear counterparts.

Here, we present the effects of crosslinker flexibility on the formation of star polymers using the arm first approach. The flexibility–performance relationship observed across the crosslinkers may inform future crosslinker design. The star polymers formed throughout this study are unique due to the high rigidity, length, and MW of their polywedge arms. We find trends relating arm MW and crosslinker ratio to arm conversion and arms per star. Finally, we experimentally verify the scaling relationship of size and MW for the linear and star polymers predicted from a previous theoretical analysis.[47–49]

EXPERIMENTAL

Syntheses
All chemicals were purchased from Sigma-Aldrich or VWR, unless otherwise reported. All polymerizations were carried out inside a nitrogen filled glovebox.

ROMP Catalyst (1) ((H$_2$IMes) (py)$_2$(Cl)$_2$RuCHPh)
(H$_2$IMes) (PPh$_3$) (Cl)$_2$RuCHPh was received as a research gift from Materia, Inc. and was converted to (H$_2$IMes) (py)$_2$(Cl)$_2$RuCHPh (1) via literature procedure.[50]

Benzyl Wedge (2)
Benzyl wedge monomer (BnW) was prepared via literature procedure.[40]

1,10-Di-Norbornene Decane (3$_A$)
2.2 Equivalents of *cis*-5-norbornene-*exo*-2,3-dicarboxylic anhydride (*exo*-norbornene) (500 mg, 3.05 mmol) and 1 equivalent of 1,10-diaminodecane (240 mg, 1.39 mmol), neat, were stirred at 140 °C in a sealed, thick-walled glass flask for 60 min. After the reaction cooled, CH$_2$Cl$_2$ was added to form a concentrated solution which was filtered through a plug of silica. The resulting product was dried by rotary evaporation and crystallized from diethyl ether. The crystals

were isolated by filtration and dried overnight *in vacuo*. Yield 20% (129 mg). ^{1}H NMR (300 MHz, CDCl$_3$) δ 6.23 (t, $J = 1.9$ Hz, 4H), 3.45–3.33 (m, 4H), 3.22 (p, $J = 1.7$ Hz, 4H), 2.62 (d, $J = 1.4$ Hz, 4H), 1.55–1.39 (m, 6H), 1.31–1.08 (m, 15H). ^{13}C (75 MHz, CDCl$_3$) δ 178.1, 137.9, 47.82, 45.19, 44.93, 42.75, 38.75, 29.33, 29.09, 27.78, 26.95.

Para-*Xylene Dinorbornene (3$_B$)*
A 100 mL thick-walled flask was equipped with a stir bar and flame-dried under vacuum. Once cooled, the flask was back filled with nitrogen and 2.2 equivalents of *cis*-5-norbornene-*exo*-2,3-dicarboxylic anhydride (*exo*-norbornene) (500 mg, 3.05 mmol) and 1 equivalent of *para*-xylenediamine (189 mg, 1.39 mmol) were added. DMF (10 mL), purified using an MBRAUN solvent system, was added without further treatment and the reaction was stirred at reflux (160 °C) overnight. Overnight, a white solid formed in the DMF solution. The solid was separated by filtration and dried *in vacuo*. Yield 60% (357 mg). ^{1}H NMR (300 MHz, CDCl$_3$) 7.30 (s, 4H), 6.27 (t, $J = 1.9$ Hz, 4H), 3.24 (p, $J = 1.7$ Hz, 4H), 2.67 (d, $J = 1.4$ Hz, 4H), 1.40 (dt, $J = 9.9$, 1.6 Hz, 2H), 1.03 (ddt, $J = 10.0$, 1.6, 0.9 Hz, 2H). ^{13}C NMR (75 MHz, CDCl$_3$) δ 177.8, 138.1, 135.7, 129.3, 47.96, 45.44, 42.81, 42.12.

Para-*Phenylene Dinorbornene (3$_C$)*
A 100 mL thick-walled flask was equipped with a stir bar and flame-dried under vacuum. Once cooled, the flask was back filled with nitrogen and 2.2 equivalents of *cis*-5-norbornene-*exo*-2,3-dicarboxylic anhydride (*exo*-norbornene) (500 mg, 3.05 mmol) and 1 equivalent of *para*-phenylenediamine (150 mg, 1.39 mmol) were added. DMF (10 mL), purified using an MBRAUN solvent system, was added without further treatment and the reaction was stirred at reflux (160 °C) overnight. Overnight, a white solid formed in the DMF solution. The solid was separated by filtration and dried to pearlescent flakes *in vacuo*. Yield 63% (345 mg). ^{1}H NMR (300 MHz, CDCl$_3$) δ 7.42 (s, 4H), 6.35 (t, $J = 1.9$ Hz, 4H), 3.41 (p, $J = 1.8$ Hz, 4H), 2.86 (d, $J = 1.3$ Hz, 4H), 1.62 (dt, $J = 9.9$, 1.6 Hz, 2H), 1.45 (dt, $J = 9.9$, 1.5 Hz, 2H). ^{13}C NMR (75 MHz, CDCl$_3$) δ 176.8, 138.2, 131.9, 127.0, 77.58, 77.16, 76.74, 48.02, 46.05, 43.16.

Homo(BnW) (4)
Homo(BnW) was prepared via literature procedure.[40] Solutions of catalyst (1) were rapidly added to vigorously stirring tetrahydrofuran solutions of BnW monomer. One hour after the addition of catalyst, the homo(BnW) solution was diluted to facilitate precise and convenient aliquots for the following star polymer synthesis.

Star(Homo(BnW)) (5)
The mass of crosslinker required to achieve the desired crosslinker to arm molar ratio was dissolved with DCM (4 mL) in a 20 mL vial with a poly(ethylene) lining on the cap and stirred vigorously. One hour after the addition of catalyst to the monomer solution, 1 mL aliquots from the polymer solution were added rapidly to the stirring crosslinker solution. After 2, 6, or 24 h, the reaction was

quenched by the addition of ethyl vinyl ether (150 μL). Star polymers were isolated by drying the mixture to a saturated solution, precipitating with the addition of methanol (MeOH) (10 mL), and filtering and washing the resulting solid with MeOH. The star polymer products were dried in a vacuum oven at 50 °C overnight.

Analyses

Gel Permeation Chromatography with Multi-Angle Light Scattering (GPC-MALS)

Polymer molecular weights were determined by gel permeation chromatography (GPC) coupled with multiangle light-scattering (MALS), using an Agilent HPLC fitted with one PLgel 5 μm guard column and three PLgel 5 μm MIXED-C gel permeation columns, a Wyatt Technology TrEX differential refractometer, and a Wyatt Technology miniDAWN TREOS light scattering detector, using THF as the eluent at a flow rate of 1.0 mL/min. Absolute molecular weights were determined using dn/dc values calculated by assuming 100% mass recovery of the polymer sample with a known concentration injection onto the GPC. The dn/dc of homo(BnW) is 0.1702, calculated as an average of 3 different molecular weights and concentrations. The dn/dc of the star polymers was calculated using the known dn/dc of the homopolymer arms. First, the mass of the unreacted arms was calculated. The residual mass, consistent with the 100% mass recovery assumption, was used to calculate the dn/dc of the stars. This method was applied to 5 different star polymer products and the results were averaged, yielding a dn/dc for star(homo(BnW)) of 0.2116.

Number-Average Root Mean Square Radius (R_n)

The radii were calculated from dilute solutions ($<$1 mg/mL) of star polymers and a Wyatt Technology miniDAWN TREOS light scattering detector using THF as the eluent at room temperature.

Nuclear Magnetic Resonance (NMR) Characterization

NMR spectra were recorded on Bruker 300 MHz spectrometer. Chemical shifts were referenced to internal solvent resonances using CDCl$_3$ (^{1}H: 7.26 ppm; ^{13}C: 77.16 ppm) and are reported as parts per million relative to tetramethylsilane.

RESULTS AND DISCUSSION

Crosslinker Comparison

As crosslinker flexibility was hypothesized to influence the efficiency of star formation, three crosslinkers were designed with varying levels of flexibility between the anhydrous *cis*-5-norbornene-*exo*-2,3-dicarboxylic anhydride (*exo*-norbornene) groups. By reacting decane (R$_A$), *para*-xylene (R$_B$), and *para*-phenylene (R$_C$) diamines with *exo*-norbornene [Fig. 1(B)], three di-functional compounds were synthesized and investigated as crosslinkers (**3$_A$**, **3$_B$**, and **3$_C$**). **3$_A$** is composed of nine C—C single bonds that impart a high degree of conformational freedom between the *exo*-norbornene functionalities. In comparison, **3$_C$** is rigid, with only a phenyl ring connecting the norbornene groups. To test the capacity of the crosslinkers to form star polymers, homo(benzyl wedge)

(homo(BnW), **4**) was synthesized via ROMP and added to crosslinker *in situ*. The resulting products were analyzed by GPC coupled with multi-angle light scattering (MALS) (Table 1). Across a wide range of molecular weights and through variation of the ratio of crosslinker to polymer, **3$_C$** consistently achieved the highest star weight-average molecular weight (M_w) and mass conversion. **3$_A$** failed to achieve higher than 10% mass conversion and forms mostly dimeric species.

The GPC-MALS analysis reveals the non-equivalent ability of each crosslinker to produce star polymers (Fig. 2). When the most flexible crosslinker (**3$_A$**) is added, the star polymer product peak has a low intensity; only 5.7% of the polymer arms are converted to predominantly two-arm products. Using the crosslinker with intermediate flexibility (**3$_B$**) in a similar reaction results in 52% of the polymer arms converting to star polymers with mostly two to three arms. When the most rigid crosslinker (**3$_C$**) is used, 76% of the polymer arms react to form star polymers with up to four arms. As shown in Table 1, for all M_w and ratios of crosslinker to arms, the star polymers produced when using **3$_C$** have higher M_w's than the products from reactions with either **3$_A$** or **3$_B$**. **3$_C$** is the most effective at forming star polymers with the highest conversions and with the most arms per star. Upon addition to the polymerization solution, the crosslinkers react with the active catalyst (**1**) on the end of **4**. Because **3** is di-functional, there is an unpolymerized *exo*-norbornene group for each added molecule of **3**. The unpolymerized *exo*-norbornenes continue to react with **3** or **4** in unpolymerized *exo*-norbornenes forming the star polymer product (**5**).

When low-MW (degree of polymerization (DP) $<$150) arms are reacted with any of the crosslinkers, complete consumption of both *exo*-norbornene functionalities on the crosslinker is observed through the disappearance of norbornene double bonds by ^{1}H NMR analysis of the star polymers (see Figs. S11, S14, and S16). No low-MW signal appears on the GPC traces of polymer products after the addition of **3**, indicating homo(**3**) does not form in solution. The added crosslinker is largely incorporated into the core of **5** and **3** has reacted with either additional **3** or **4**. Despite the nearly complete polymerization of crosslinker in the product, each crosslinker tested produced incomplete conversion to star polymers, shown by the presence of the arm peak on the GPC traces. Once the crosslinker in solution has been incorporated into the core, a pathway arises to cease polymerization and explain these two observations. If an *exo*-norbornene within the core reacts with an active site on the end of a chain, it will polymerize without adding additional **3** or **4** to the chain. Once this poly(**3**) cyclization occurs, there are no remaining unreacted norbornene functionalities, preventing new polymer arms or polymer arm-crosslinker compounds from binding to the star polymer. Poly(**3**) cyclization has been reported previously as a limiting factor in brush-first star synthesis.[34] Crosslinker flexibility increases the likelihood of the intramolecular cyclization events that prevent the further formation of star polymers. The reaction
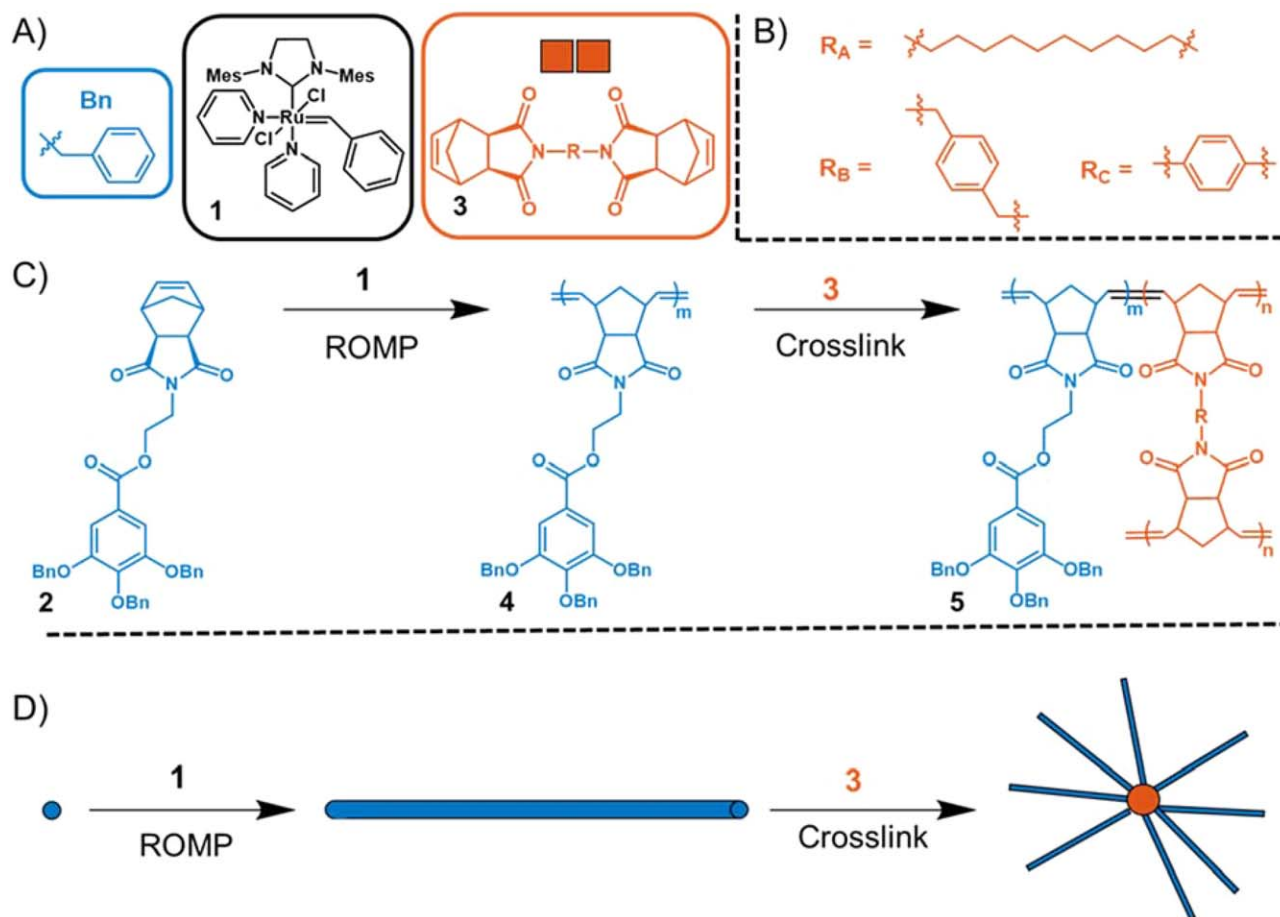
FIGURE 1 (A) Structure of the ROMP catalyst (1) (Mes = mesitylene), benzyl wedge monomer (BnW, 2), and a generic crosslinker (3). (B) Chemical core of the different crosslinkers investigated in this study. (C) Reaction scheme for synthesis of homo(BnW) (4) and star(homo(BnW)) (5) from 2. (D) A schematic of the synthetic approach and the resulting linear and star polymers. [Color figure can be viewed at wileyonlinelibrary.com]

between **3** and **4** is limited by the slow diffusion rate of the large polymer arms, allowing many intramolecular cyclization events to occur.

In addition, for high-MW (DP >150) arms reacted with 3_B and 3_C, there are no unpolymerized crosslinker present by NMR analysis. 3_A, however, presents an exception. When 3_A was reacted with low-DP arms (DP = 98, $M_w = 58$ kDa), every exo-norbornene group polymerized and participated in the reaction. In comparison, when reacted with high-DP arms (DP = 227, $M_w = 133$ kDa), approximately 28% of the exo-norbornene groups remained unpolymerized (Figs. S11 and S12). This incomplete conversion is most likely due to a combination of two factors: the flexibility of the crosslinker and the increased steric bulk of the high MW polywedge arms. The rapid addition of decane-containing crosslinkers to the growing polymer chain creates a high local concentration of flexible decane spacers. Some of these decane spacers become entangled with one another,[51] creating trapped exo-norbornene groups inside the forming core. These groups are rendered inaccessible to additional polymer arms by the combination of trapped end groups and bulky polywedge

arms, preventing further arms from reacting with the available exo-norbornene functionalities. The steric hindrance in the system results in norbornene groups that stay unpolymerized but react extremely slowly or not at all, which is observed via GPC (Fig. 3).

To further test the hypothesis that crosslinker flexibility hinders star formation and arm incorporation, a reaction of each crosslinker with various polymer M_w and crosslinker ratios was monitored for 24 h. Analysis by GPC-MALS reveals that regardless of the polymer M_w or the amount of crosslinker, the reaction proceeds at a dramatically slower rate (3_A) or ceases to proceed (3_B and 3_C) within 2 h of crosslinker addition (Fig. 3). This result confirms that the available norbornene species react rapidly when added to the polymer solution. The rapid reaction of exo-norbornene functionalities on the crosslinkers ultimately leads to intra-core polymerization events, ending the growth of individual macromolecules. A crosslinker that can rotate freely – such as 3_A – is more likely to participate in cyclization events, rapidly ceasing polymerization, and producing star polymers in lower yield.

TABLE 1 Summary of Star Polymer Synthesis Using 3_A, 3_B, and 3_C Crosslinkers

3_A							
Arm M_w (kDa)[a]	Arm $Đ$ (M_w/M_n)	$[R_A]$:$[4]$[b]	Star M_w (kDa)[a]	Star $Đ$ (M_w/M_n)	Mass Conv. (%)[a]	# of Arms[c]	R_n (nm)[d]
57.8	1.01	5.8	111	1.02	2.0	1.9	7.2
57.8	1.01	23	123	1.02	5.7	2.0	9.1
133	1.02	6.7	207	1.02	1.9	1.5	13
133	1.02	27	230	1.02	3.8	1.6	14
232	1.01	5.4	395	1.06	0.5	1.7	19
232	1.01	22	412	1.01	1.4	1.7	21
3_B							
Arm M_w (kDa)[a]	Arm $Đ$ (M_w/M_n)	$[R_B]$:$[4]$[b]	Star M_w (kDa)[a]	Star $Đ$ (M_w/M_n)	Mass Conv. (%)[a]	# of Arms[c]	R_n (nm)[d]
28.8	1.01	7.1	62.3	1.08	53	2.1	-
28.8	1.01	28	94.3	1.10	68	2.9	3.0
40.0	1.01	13	68.8	1.17	43	1.7	-
40.0	1.01	25	90.3	1.07	52	2.3	4.4
40.0	1.01	50	100	1.08	59	2.5	5.6
101	1.00	10	180	1.05	22	1.8	11
101	1.00	20	201	1.05	27	2.0	11
101	1.00	34	216	1.07	30	2.1	11
124	1.01	7.0	225	1.02	18	2.6	14
124	1.01	28	258	1.05	32	2.9	13
3_C							
Arm M_w (kDa)[a]	Arm $Đ$ (M_w/M_n)	$[R_C]$:$[4]$[b]	Star M_w (kDa)[a]	Star $Đ$ (M_w/M_n)	Mass Conv. (%)[a]	# of Arms[c]	R_n (nm)[d]
28.8	1.01	7.1	137	1.14	82	4.6	4.0
28.8	1.01	28	341	1.11	92	11	6.9
40.0	1.01	25	154	1.13	76	3.9	6.3
40.0	1.01	50	249	1.07	81	6.2	7.3
101	1.01	10	562	1.09	59	5.6	15
101	1.01	20	870	1.09	76	8.6	17
101	1.01	40	1090	1.07	89	11	16
124	1.01	7.0	336	1.09	39	2.7	17

[a] Determined by GPC.
[b] Assumes 100% conversion from BnW monomer to homo(BnW).
[c] Determined by light scattering, adjusted to account for the added mass of the crosslinker.
[d] Number average root mean square radius, determined by MALS.

Effect of Polymer Arm Molecular Weight

Illustrated in Figure 3 and Table 1, the MW of the polywedge arms has a pronounced effect on the ability of any crosslinker to produce star polymers. The mass conversion of polymer arms to star polymers decreases as polymer arm MW increases. A similar result is observed as the molar amount of crosslinker decreases. To investigate these dependencies, 3_C, which preliminary testing determined to give the highest conversion, was reacted with homo(BnW) arms over a wide range of MWs and crosslinker ratios. Aliquots from a polymerization solution with active catalyst were added to vials of crosslinker solutions at different concentrations. This process assessed the formation of stars from a wide range of polymer arm M_w (from 101 kDa to 805 kDa) and molar ratios of crosslinker to polymer arm (from 10 to 233) (Fig. 4 and Table S1). GPC analysis shows that both mass conversion and the number of arms per star increased logarithmically as the molar equivalents of crosslinker are increased. The logarithmic response plateaued more quickly for polymer arms with higher MW.

It is worth noting that these two metrics could be independent. For example, a possible outcome of adding more crosslinker could be to form more dimers, increasing mass conversion but not arms per star. However, in this system, the mass conversion and number of arms follow the same trend: as the conversion increases, there are both fewer unreacted arms and more arms per star. This behavior is revealed by GPC traces of polymer products formed by reacting the same homo(BnW) arms with various ratios of crosslinker (Fig. 5). The increase in crosslinker equivalents simultaneously reduces the intensity of the arm peak and
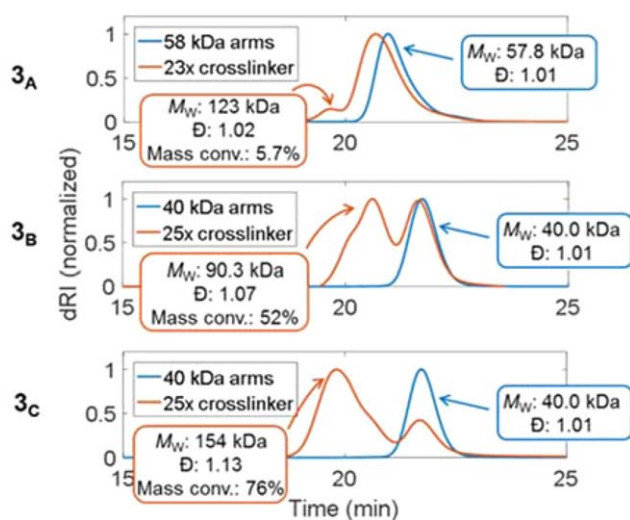
FIGURE 2 GPC traces for star polymers produced by reacting similar molar ratios of 3_A, 3_B, and 3_C with homo(BnW) polywedges of similar molecular weights. The red traces were taken after the crosslinking reaction had proceeded for 2 h. [Color figure can be viewed at wileyonlinelibrary.com]

causes the product to elute earlier, showing a star with higher MW and more arms. The preceding analyses were performed on the crude reaction product (e.g., aliquots).

Decrease in conversion and arms per star is a direct result of the increase in MW of the polymer arms. Recent research on star polymers has reported the poor ability of arms with a large DP to form star polymers with high conversion and

many arms per star.[16] Specifically, a marked decrease in mass conversion as the DP of a polymer arm exceeded 150 is noted. The polymer arms in this study (Fig. 4) had DPs ranging from 171 (101 kDa, green) to 1370 (805 kDa, purple) and the conversion-diminishing effect of MW was pronounced (92–55% conversion, at a crosslinker ratio of 85:1) within that range. The previous study fixed crosslinker equivalents at 14, so to the best of our knowledge there are no previous results for star polymers formed from high DP arms with the high crosslinker equivalents used here. We suspect the same phenomena cited previously are responsible for the behavior observed here: long polymer chains have lower mobility in solution and sterically hinder the incorporation of additional arms. Increased chain length lowers the rate at which polymer arms attach to the core, biasing the core composition further toward crosslinker-crosslinker bonds. The slower diffusion and steric bulk of the large polymer arms obstruct the incorporation of successive arms, resulting in lower mass conversion and fewer arms per star. As shown in this work, an increase in crosslinker equivalents results in increased star polymer yield and higher DP arms require more crosslinker to reach the same yields obtained with lower DP arms.

Conformation of Polymer Arms and Product in Solution

A polymer's conformation in solution can be elucidated from how a change in molecular weight changes the polymer's size. These two metrics are related by the scaling exponent, determined by plotting M_w against radius. This analysis is shown for both the homo(BnW) polymer arms and the star polymer products (Fig. 6).
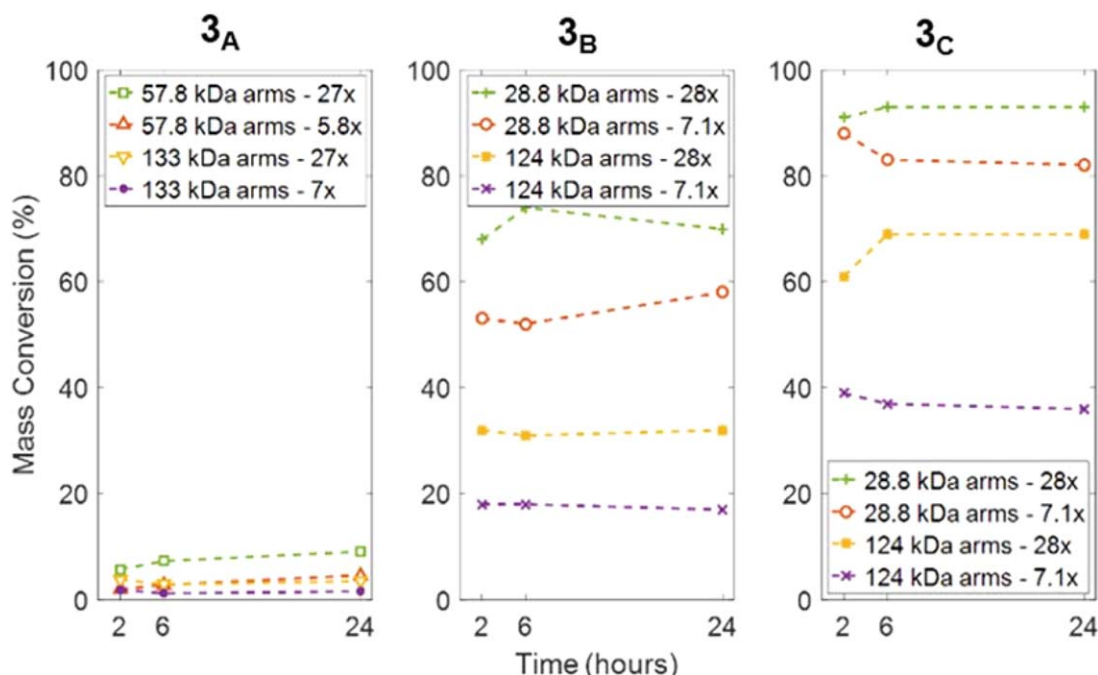

FIGURE 3 Plots of mass conversion as a function of time for linear homo(BnW) reacted with 3_A, 3_B, and 3_C crosslinkers with similar polymer arm M_w and crosslinker concentrations after 2, 6, and 24 h. The legend states the M_w of the polymer arm and the molar equivalents of crosslinker used. [Color figure can be viewed at wileyonlinelibrary.com]
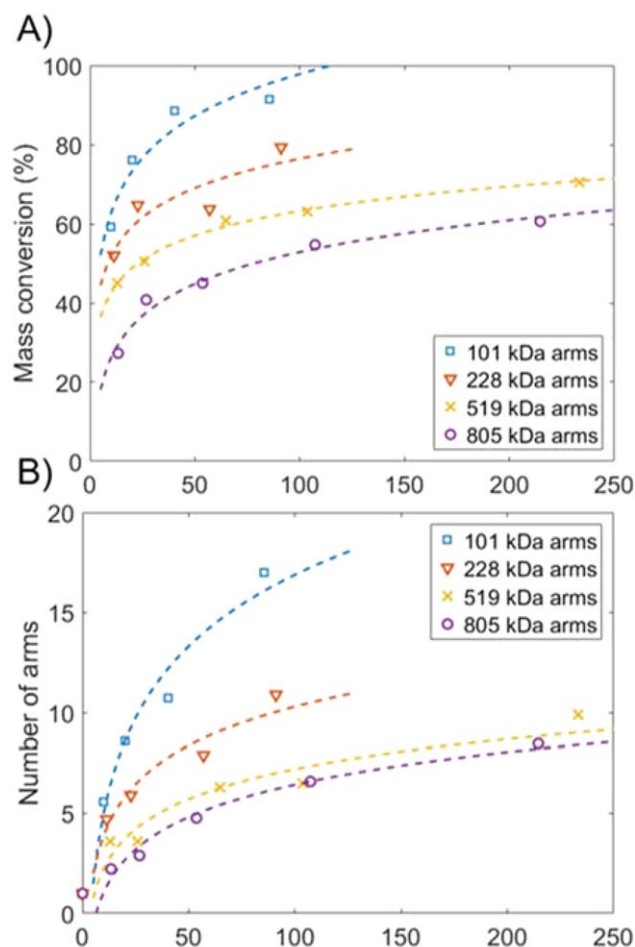
FIGURE 4 Plots of (A) mass conversion and (B) number of arms incorporated as a function of molar equivalence of **3$_C$** added. The open markers show the data points; the dashed lines show a logarithmic fit. [Color figure can be viewed at wileyonlinelibrary.com]

Figure 6(A) log–log plots of homo(BnW) M_w series against the number average radius, R_n. The markers represent experimental data; the dashed line represents the power fit. The slope of the fitted lines, which reveals the molecular conformation in solution, is 0.90 for the homo(BnW). The guideline drawn (black) is for ideal rigid-rod polymers (slope = 1). Figure 6(B) Log–log plots of the M_w against number average radius for the linked product produced by reacting **3$_C$** with arms of different molecular weights. The markers represent experimental data; the dashed line represents the power fit. The calculated slopes are 0.13 (101 kDa arms, green), 0.32 (225 kDa arms, red), 0.14 (527 kDa arms, yellow), and 0.21 (805 kDa arms, purple). The guidelines drawn are for hard-sphere polymers (slope = 1/3) and star polymers with a small number of very long arms (slope = 1/5).[47]

A polymer which behaves like an ideal rigid rod in solution only expands in one dimension as mass is added. Accordingly, a rigid rod would have a scaling exponent of 1.0. The BnW monomer was designed to polymerize into a rigid rod

and discourage chain entanglement.[40,42] The analysis relating M_w and number average root mean square radius (R_n) shows the polymer arms coil very little in solution; instead they rapidly gain length as weight is added. These results determine the scaling exponent for homo(BnW) to be 0.90 ($R^2 = 0.83$).

For the star polymers, the same analysis reveals scaling exponents that are much lower; the star polymer size increases very slowly as mass is added. Theoretical results predict that the scaling exponent for star polymers in a good solvent to be 1/5.[47] This prediction only holds for star polymers where the arms are very long and the number of arms is small, which is a regime into which all star polymers in our study fall. The experimentally measured values for these exponents range from 0.13 to 0.32 (see Fig. S19 for all equations and corresponding R^2 values). The calculated scaling exponents for star polymers with different MW arms are subject to errors in measurement due to the polydispersity of the star polymer products, but average to 1/5. The scaling exponents are lower than the value for a hard sphere (1/3), but in line with the results predicted by theory for stars with a small number of large arms (1/5). To our knowledge, this work is the first experimental result directly verifying these predictions for polymers with few (<20) arms.[25]

The radius of the star polymer is dictated by the length of the arms, not directly by the M_w. For example, doubling the number of arms from 4 to 8 dramatically changes the density of the star polymer, but not the volume. To explain the slight increase in radius, the role solvent plays in conformation must be considered. THF is a good solvent for these polymers; the monomers thermodynamically prefer to be surrounded by solvent over other monomer units. As the star polymer incorporates more arms, the volume near the core becomes congested and those monomers near the center are brought closer to other polymer chains. Consequently, the arms expand further to maximize their contact with the solvent. The extension of the arms as additional arms are added causes the slight radius increase seen as a function of
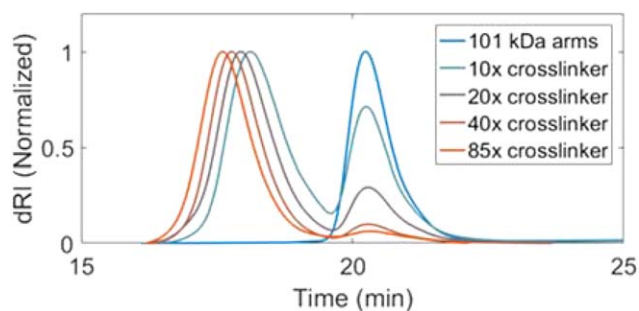

FIGURE 5 Overlaid GPC traces of the 101 kDa arms (green curve, Fig. 4) reacted with different molar amounts of the **3$_C$** crosslinker. All product traces were collected after the crosslinking reaction had proceeded for 2 h. [Color figure can be viewed at wileyonlinelibrary.com]
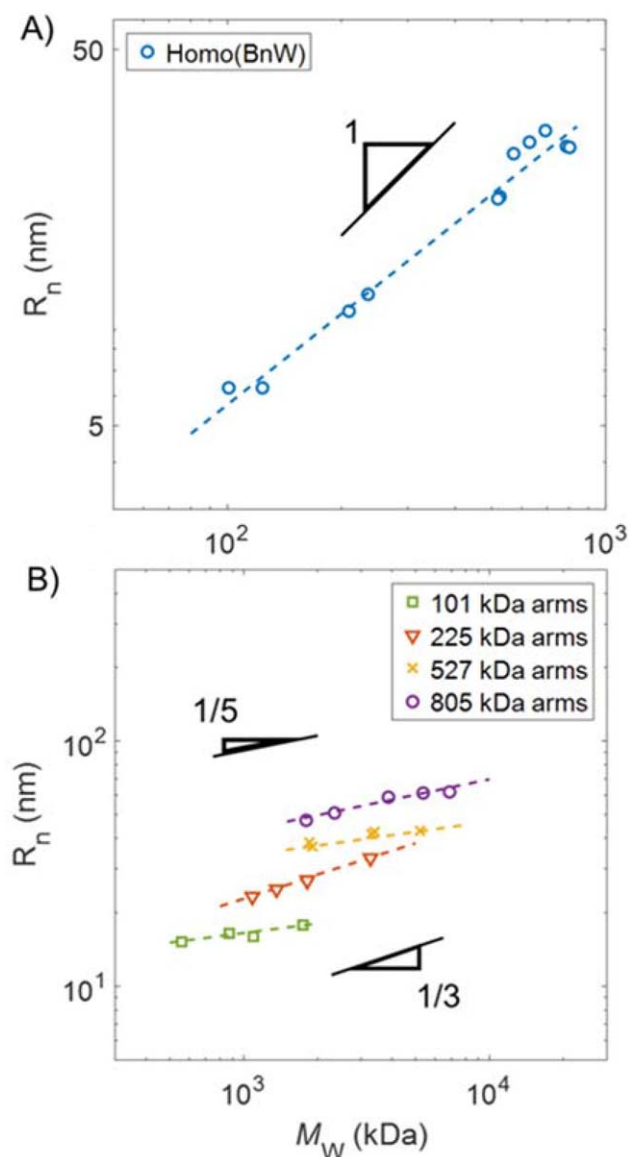
FIGURE 6 (A) Log–log plots of homo(BnW) M_w series against the number average radius, R_n. The markers represent experimental data; the dashed line represents the power fit. The slope of the fitted lines, which reveals the molecular conformation in solution, is 0.90 for the homo(BnW). The guideline drawn (black) is for ideal rigid-rod polymers (slope = 1). (B) Log–log plots of the M_w against number average radius for the linked product produced by reacting 3_C with arms of different molecular weights. The markers represent experimental data; the dashed line represents the power fit. The calculated slopes are 0.13 (101 kDa arms, green), 0.32 (225 kDa arms, red), 0.14 (527 kDa arms, yellow), and .21 (805 kDa arms, purple). The guidelines drawn are for hard-sphere polymers (slope = 1/3) and star polymers with a small number of very long arms (slope = 1/5).[47] [Color figure can be viewed at wileyonlinelibrary.com]

star polymer MW. As the individual polywedge arms are nearly fully extended before they are incorporated into the star, the potential for increase in radius is small.

CONCLUSIONS

Three bifunctional crosslinkers have been designed and synthesized and used to form star polymers from polywedge arms. The most rigid crosslinker was determined to provide the highest conversion and arms per star across a wide range of high polymer arm MWs. A logarithmic response in conversion and arm incorporation was observed as the ratio of crosslinker to arms was increased. Increasing polymer arm MW was discovered to discourage star polymer formation, corroborating previous results. The relationship between polymer size in solution and polymer MW was determined for the linear and star polymers and the slight increases in size with star polymer MW verified previous theoretical results. This ability to synthesize arm-first star polymers from polywedges will facilitate the future development of polymeric materials with unique macroscopic behavior.

REFERENCES AND NOTES

1 J. Roovers, L. L. Zhou, P. M. Toporowski, M. van der Zwan, H. Iatrou, N. Hadjichristidis, *J. Macromol.* **1993**, *26*, 4324.

2 J. Roovers, P. Toporowski, J. Martin, *Macromolecules* **1989**, *22*, 1897.

3 S. Bywater, *Adv. Polym. Sci.* **1979**, *30*, 89.

4 F. Wenger, *J. Phys. Chem.* **1963**, *67*, 566.

5 D. Vlassopoulos, G. Fytas, T. Pakula, J. Roovers, *J. Phys. Condens. Matter* **2001**, *13*, R855.

6 M. Morton, T. E. Helminiak, S. D. Gadkary, F. Bueche, *J. Polym. Sci.* **1962**, *57*, 471.

7 J. M. Ren, T. G. McKenzie, Q. Fu, E. H. H. Wong, J. Xu, Z. An, S. Shanmugam, T. P. Davis, C. Boyer, G. G. Qiao, *Chem. Rev.* **2016**, *116*, 6743.

8 G. Lapienis, *Prog. Polym. Sci.* **2009**, *34*, 852.

9 J. M. Ren, Q. Fu, A. Blencowe, G. G. Qiao, *ACS Macro Lett.* **2012**, *1*, 681.

10 L. Xue, U. S. Agarwal, P. J. Lemstra, *Macromolecules* **2005**, *38*, 8825.

11 F. Wang, T. K. Bronich, A. V. Kabanov, R. D. Rauh, J. Roovers, *Bioconjug. Chem.* **2005**, *16*, 397.

12 W. Yuan, J. Yuan, S. Zheng, X. Hong, *Polymer (Guildf)* **2007**, *48*, 2585.

13 H. Gao, *Macromol. Rapid Commun.* **2012**, *33*, 722.

14 X. Pang, L. Zhao, W. Han, X. Xin, Z. Lin, *Nat. Nanotechnol.* **2013**, *8*, 426.

15 D. C. Forman, F. Wieberger, A. Gröschel, A. H. E. Müller, H.-W. Schmidt, C. K. Ober, *Proc. SPIE* **2010**, *7639*, 76390P.

16 H. Ding, S. Park, M. Zhong, X. Pan, J. Pietrasik, C. J. Bettinger, K. Matyjaszewski, *Macromolecules* **2016**, *49*, 6752.

17 H. Gao, K. Matyjaszewski, *Prog. Polym. Sci.* **2009**, *34*, 317.

18 J. Xia, X. Zhang, K. Matyjaszewski, *Macromolecules* **1999**, *32*, 4482.

19 K. Nomura, Y. Watanabe, S. Fujita, M. Fujiki, H. Otani, *Macromolecules* **2009**, *42*, 899.

20 T. Ooya, J. Lee, K. Park, *J. Control. Release* **2003**, *93*, 121.

21 Q. Qiu, G. Liu, Z. An, *Chem. Commun.* **2011**, *47*, 12685.

22 B. V. K. J. Schmidt, T. Rudolph, M. Hetzer, H. Ritter, F. H. Schacher, C. Barner-Kowollik, *Polym. Chem.* **2012**, *3*, 3139.

23 O. Altintas, B. Yankul, G. Hizal, U. Tunca, *J. Polym. Sci. Part A: Polym. Chem.* **2006**, *44*, 6458.

24 N. Hadjichristidis, *J. Polym. Sci. Part A: Polym. Chem.* **1999**, *37*, 857.

25 T. K. Goh, K. D. Coventry, A. Blencowe, G. G. Qiao, *Polymer (Guildf)* **2008**, *49*, 5095.

26 C. N. Likos, H. Löwen, M. Watzlawek, B. Abbas, O. Jucknischke, J. Allgaier, D. Richter, *Phys. Rev. Lett.* **1998**, *80*, 4450.

27 M. Watzlawek, C. N. Likos, H. Löwen, *Phys. Rev. Lett.* **1999**, *82*, 5289.

28 H. Gao, K. Matyjaszewski, *Macromolecules* **2007**, *40*, 399.

29 M. Stenzel-Rosenbaum, T. P. Davis, V. Chen, A. G. Fane, *J. Polym. Sci. Part A: Polym. Chem.* **2001**, *39*, 2777.

30 T. Shibata, S. Kanaoka, S. Aoshima, *J. Am. Chem. Soc.* **2006**, *128*, 7497.

31 I. Bellin, S. Kelch, R. Langer, A. Lendlein, *Proc. Natl. Acad. Sci.* **2006**, *103*, 18043.

32 J. M. Ren, J. T. Wiltshire, A. Blencowe, G. G. Qiao, *Macromolecules* **2011**, *44*, 3189.

33 J. T. Wiltshire, G. G. Qiao, *Macromolecules* **2006**, *39*, 4282.

34 J. Liu, A. O. Burts, Y. Li, A. V. Zhukhovitskiy, M. F. Ottaviani, N. J. Turro, J. A. Johnson, *J. Am. Chem. Soc.* **2012**, *134*, 16337.

35 A. O. Burts, A. X. Gao, J. A. Johnson, *Macromol. Rapid Commun.* **2014**, *35*, 168.

36 R. S. Saunders, R. E. Cohen, S. J. Wong, R. R. Schrock, *Macromolecules* **1992**, *25*, 2055.

37 A. Leitgeb, J. Wappel, C. Slugovc, *Polymer (Guildf)* **2010**, *51*, 2927.

38 G. M. Miyake, R. A. Weitekamp, V. A. Piunova, R. H. Grubbs, *J. Am. Chem. Soc.* **2012**, *134*, 14249.

39 R. J. Macfarlane, B. Kim, B. Lee, R. A. Weitekamp, C. M. Bates, S. F. Lee, A. B. Chang, K. T. Delaney, G. H. Fredrickson, H. A. Atwater, R. H. Grubbs, *J. Am. Chem. Soc.* **2014**, *136*, 17374.

40 V. A. Piunova, G. M. Miyake, C. S. Daeffler, R. A. Weitekamp, R. H. Grubbs, *J. Am. Chem. Soc.* **2013**, *135*, 15609.

41 M. Hu, Y. Xia, C. S. Daeffler, J. Wang, G. B. McKenna, J. A. Kornfield, R. H. Grubbs, *J. Polym. Sci. Part B: Polym. Phys.* **2015**, *53*, 899.

42 B. M. Boyle, T. A. French, R. M. Pearson, B. G. McCarthy, G. M. Miyake, *ACS Nano* **2017**, *11*, 3052.

43 M. Hu, Y. Xia, G. B. McKenna, J. A. Kornfield, R. H. Grubbs, *Macromolecules* **2011**, *44*, 6935.

44 S. F. Rubin, R. M. Kannan, J. a. Kornfield, C. Boeffel, *Macromolecules* **1995**, *28*, 3521.

45 L. J. Fetters, D. J. Lohse, W. W. Graessley, *J. Polym. Sci. Part B: Polym. Phys.* **1999**, *37*, 1023.

46 M. G. Mayershofer, O. Nuyken, M. R. Buchmeiser, *Macromolecules* **2006**, *39*, 3484.

47 M. Daoud, J. P. Cotton, *J. Phys.* **1982**, *43*, 531.

48 M. Daoud, J. F. Joanny, *J. Phys.* **1981**, *42*, 1359.

49 B. J. Bauer, N. Hadjichristidis, L. J. Fetters, J. E. L. Roovers, *J. Am. Chem. Soc.* **1980**, *102*, 2410.

50 J. A. Love, J. P. Morgan, T. M. Trnka, R. H. Grubbs, *Angew. Chem. Int. Ed.* **2002**, *41*, 4035.

51 R. P. Wool, *Macromolecules* **1993**, *26*, 1564.